



- Taking precast concrete to the limit
- Challenges for concrete in tall buildings
- Overview of imposed deformation in concrete structures
- Appraisal of models for estimating drying shrinkage strains
- Serviceability uncertainties in flat slabs
- Punching shear tests on symmetrically reduced slab quarters
- Review of different punching shear provisions for footings
- New model for predicting FRP-concrete bond strength
- Super-light concrete floor slabs
- Monitoring-based fatigue assessment for concrete structures
- Fire performance of composite hollow column with inner tube
- Resource management of sustainable recycling concrete
- Post-installed reinforcement connections at ULS and SLS
- Behaviour of fatigue loaded self-compacting concrete vs. vibrated concrete



One of Netherland's most important north to south corridors is the A50 motorway and a part of it the Waal Bridge near Ewijk with a main span of 270 m. Build between 1971 and 1976, it is one of the longest bridge structures in the Netherlands. The Rijkswaterstaat, the executive arm of the Dutch Ministry of Infrastructure and the Environment, has decided to widen the A50 motorway between Ewijk and Valburg in both directions from two to four lanes each over a distance of 7 km. The entire project was carried out within the scope of a Design-Build contract. The consortium responsible for its execution and design is Waalkoppel, a consortium consisting of Mobilis, Van Gelder B.V. and DYWIDAG Bau GmbH. (see page A5 f)

Structural Concrete

Vol. 15 / 4

December 2014
ISSN 1464-4177 (print)
ISSN 1751-7648 (online)

Wilhelm Ernst & Sohn
Verlag für Architektur und technische
Wissenschaften GmbH & Co. KG
www.ernst-und-sohn.de

 **fib**
fédération internationale
du béton
International Federation
for Structural Concrete
www.fib-international.org

Journal of the *fib*

Peer reviewed journal

Since 2009, *Structural Concrete* is indexed
in Thomson Reuter's Web of Knowledge
(ISI Web of Science).

Impact Factor 2013: 0.857

**Wiley
Online
Library**

www.wileyonlinelibrary.com, the portal for
Structural Concrete online subscriptions

Editorial

- 439 Mette Glavind
Innovations in concrete for sustainable infrastructure constructions

Technical Papers

- 441 Kaare K. B. Dahl
Bella Sky Hotel – taking precast concrete to the limit
- 448 Gordon Clark
Challenges for concrete in tall buildings
- 454 Hans-Wolf Reinhardt
Aspects of imposed deformation in concrete structures – a condensed overview
- 461 Yvonne Theiner, Andreas Andreatta, Günter Hofstetter
Evaluation of models for estimating concrete strains due to drying shrinkage
- 469 Richard Scott
Serviceability uncertainties in flat slabs
- 484 Karsten Winkler, Peter Mark, Peter Heek, Sandra Rohländer, Simone Sommer
Punching shear tests on symmetrically reduced slab quarters
- 497 Carsten Siburg, Marcus Ricker, Josef Hegger
Punching shear design of footings: critical review of different code provisions
- 509 Majid Abdellahi, Javad Heidari, Maryam Bahmanpour
A new predictive model for the bond strength of FRP-to-concrete composite joints
- 522 Kristian Hertz, Andreas Castberg, Jacob Christensen
Super-light concrete decks for building floor slabs
- 530 Susanne Urban, Alfred Strauss, Robert Schütz, Konrad Bergmeister, Christian Dehlinger
Dynamically loaded concrete structures – monitoring-based assessment of the real degree of fatigue deterioration
- 543 Deok Hee Won, Woo Sun Park, In-Sung Jang, Sang-Hun Han, Taek Hee Han
Fire resistance performance of steel composite hollow RC column with inner tube under ISO 834 standard fire
- 556 Lamia Messari-Becker, Angelika Mettke, Florian Knappe, Ulrich Storck, Klaus Bollinger, Manfred Grohmann
Recycling concrete in practice – a chance for sustainable resource management
- 563 Norbert Randl, Jakob Kunz
Post-installed reinforcement connections at ultimate and serviceability limit states
- 575 Sara Korte, Veerle Boel, Wouter De Corte, Geert De Schutter
Behaviour of fatigue loaded self-compacting concrete compared to vibrated concrete
- 590 **2014 reviewers**
- fib-news**
- 591 Structural changes in the *fib*
- 592 60 years of setting standards
- 592 Summer studies in Milan
- 593 *fib* Bulletin 73
- 594 New *fib* Presidium
- 594 HPC conference and MC2010 workshop in Beijing
- 595 Short notes
- 596 Congresses and symposia
- 597 Acknowledgement
- A5 **Products and Projects**

Deok Hee Won
Woo Sun Park
In-Sung Jang
Sang-Hun Han
Taek Hee Han*

Fire resistance performance of steel composite hollow RC column with inner tube under ISO 834 standard fire

An internally confined hollow RC (ICH RC) column offers strong and durable confinement owing to the reinforcement provided by the inner tube. The strength and ductility of the column are enhanced because of the continuous confining stress provided by the inner tube. The excellent structural performance of ICH RC columns makes them particularly suitable for applications in high-rise buildings. However, if a high-rise building is damaged by fire, it will collapse without fire resistance performance. Also, lack of evacuation measures endangers human life. Thus, to predict the status of structures in fires, their behaviour should be evaluated in terms of fire time. In this study, the fire resistance performance of an ICH RC column was analysed during an ISO 834 standard fire and with certain initial conditions. Furthermore, the effects of hollow ratio, thickness of inner tube and thickness of cover concrete on the fire resistance performance were analysed. The results could be used for designing fire-resistant ICH RC columns.

Keywords: fire resistance, composite column, concrete, ISO 834, Eurocode

1 Introduction

Hollow RC columns are used as economical design elements because they use little material and are lightweight. However, they have poor ductility owing to brittle failure on the inner face of the column. The brittle failure of a hollow RC column originates from the lack of confinement of the core concrete because, generally, the core concrete of a hollow RC column is confined by the outer transverse reinforcement only or both the outer and the inner transverse reinforcement. To prevent this brittle failure, Han et al. [1] used an inner tube to reinforce the inner face of a hollow RC column, as shown in Fig. 1. This column is known as an internally confined hollow RC (ICH RC) column. It offers strong and durable confinement because of the reinforcement provided by the inner tube. The column's strength and ductility are enhanced because of the continuous confining stress provided by the inner tube. A non-linear concrete model and the compressive performance were analysed in an experimental study on an ICH RC column [1, 2]. In the study, the yielding and

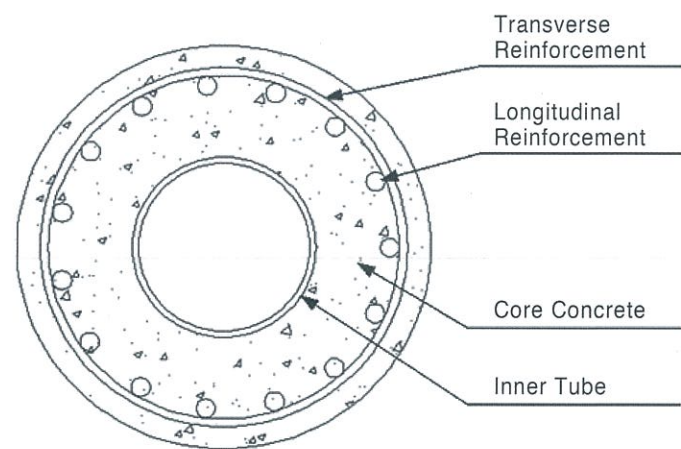


Fig. 1. Section through circular ICH RC column [1]

buckling failure conditions of the inner tube were considered as well.

The excellent structural performance of ICH RC columns makes them particularly suitable for use in high-rise buildings. However, if a high-rise building is damaged by fire, it will collapse without fire resistance performance. Also, lack of evacuation measures endangers human life [3]. Thus, for predicting the status of structures in fires, their behaviour should be evaluated in terms of fire time. In this study, the behaviour of ICH RC columns was analysed under the ISO 834 [4] standard fire. A heat transfer analysis was performed for predicting the temperature distribution due to the conduction of fire heat according to fire time. The ICH RC column's behaviour was characterized based on its temperature distribution.

2 Evaluation method for the fire resistance performance of an ICH RC column

2.1 Material properties

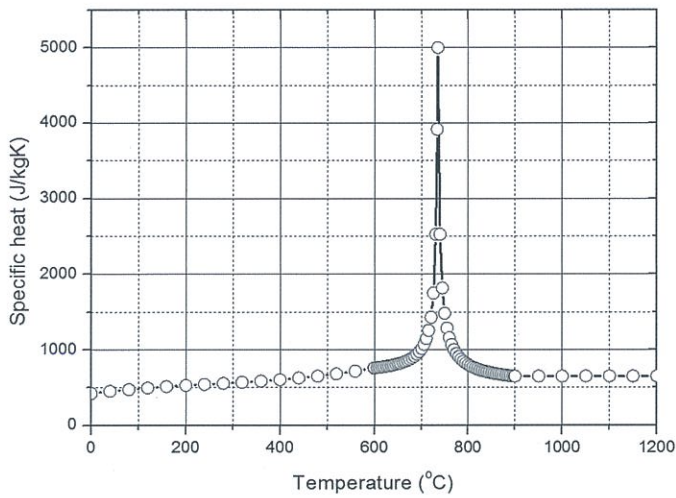
ICH RC columns consist of concrete, steel tube, transverse reinforcement and longitudinal reinforcement. To investigate column behaviour, we require material properties along with temperature. These properties can be divided into two groups: thermal material properties in terms of conduction of fire heat, and structural material properties in terms of change in material strength. The thermal material properties considered for investigating the conduc-

* Corresponding author: taekheehan@kiost.ac

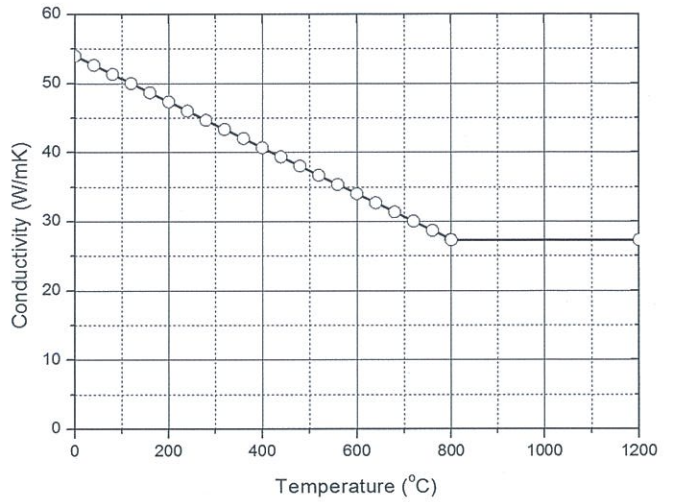
Submitted for review: 26 August 2013

Revised: 20 February 2014

Accepted for publication: 27 March 2014

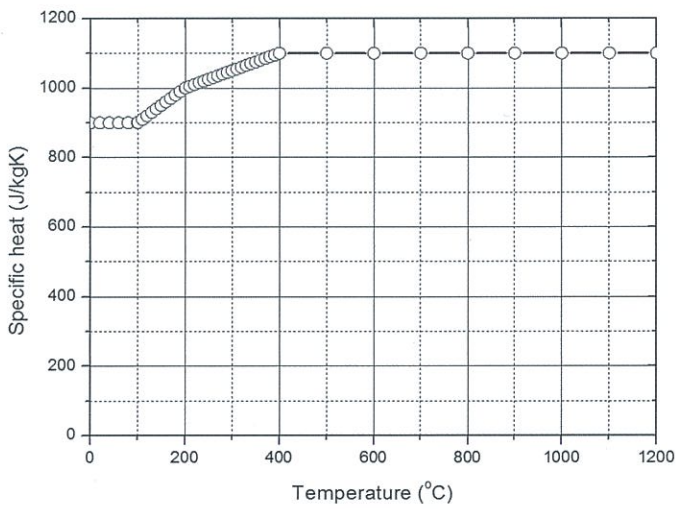


(a) Specific heat of steel

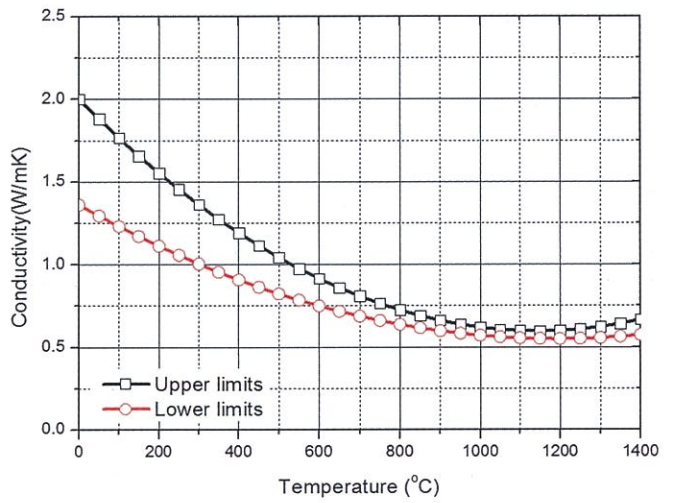


(b) Conductivity of steel

Fig. 2. Properties of steel according to Eurocode 3 [6]

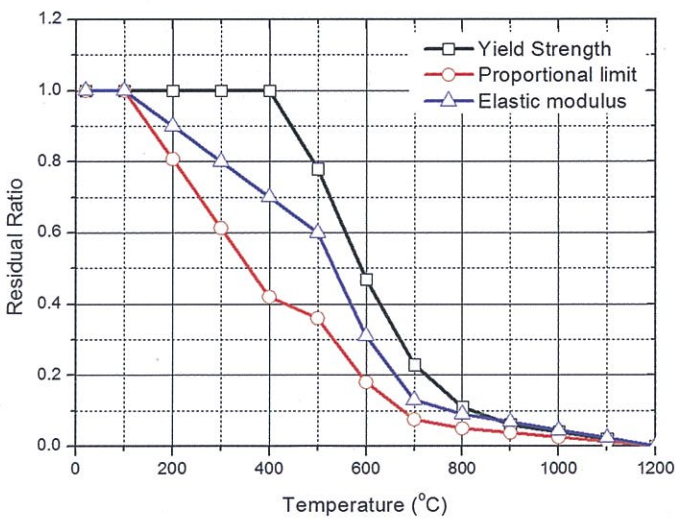


(a) Specific heat of concrete

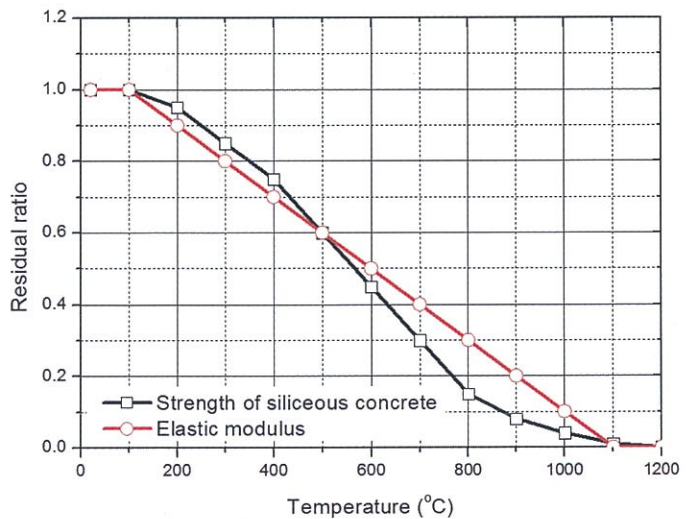


(b) Conductivity of concrete

Fig. 3. Properties of concrete according to Eurocode 2 [5]



(a) Steel properties in Eurocode 3 [6] and CEB code [7]



(b) Concrete properties in Eurocode 2 [6]

Fig. 4. Material properties in terms of temperature

tion of fire heat are representative of specific heat and conductivity. Eurocodes 2 [5] and 3 [6] list the material properties of steel and concrete respectively. Thermal material properties as shown in Figs. 2 and 3 apply for heat transfer analysis. Conductivity of concrete used the upper limit condition.

Structural material properties that depend on a change in temperature are the ultimate strength, yield strength, elastic modulus and compressive strength of concrete and steel. They are specified in Eurocodes 2 [5] and 3 [6] and in CEB code [7], as shown in Fig. 4.

2.2 Method of analysis for an ICH RC column

To predict the behaviour of an ICH RC column, a column analysis model is suggested in this study based on the Han et al. [1, 2] concrete model. This analysis tool is capable of axial load–bending moment interaction analyses. It uses section analysis, accounting for equilibrium, strain compatibility and material stress–strain curves, and adopts the layer-by-layer technique for numerical integration of stresses (Kilpatrick and Ranagan [8]). The analyses are conducted for two conditions including a) unconfined

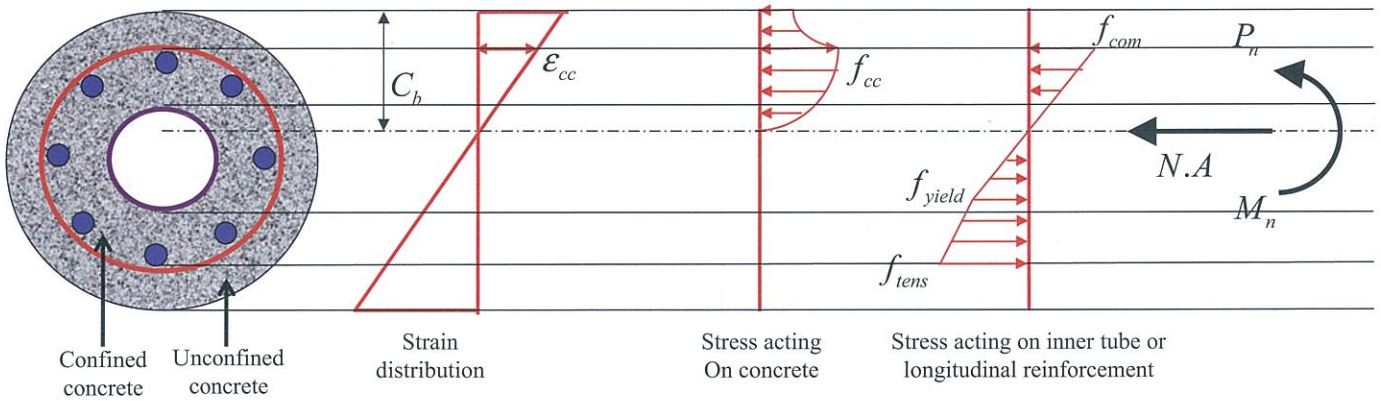


Fig. 5a. Section analysis using strain compatibility and layer-by-layer approach [2]

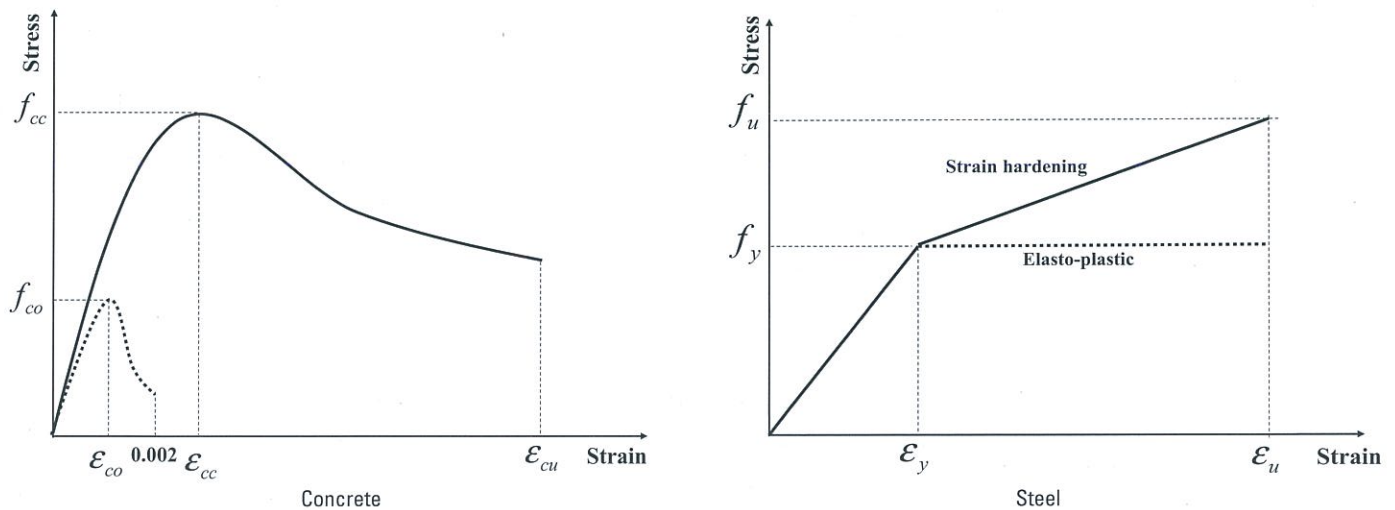


Fig. 5b. Idealized stress-strain curves [2]

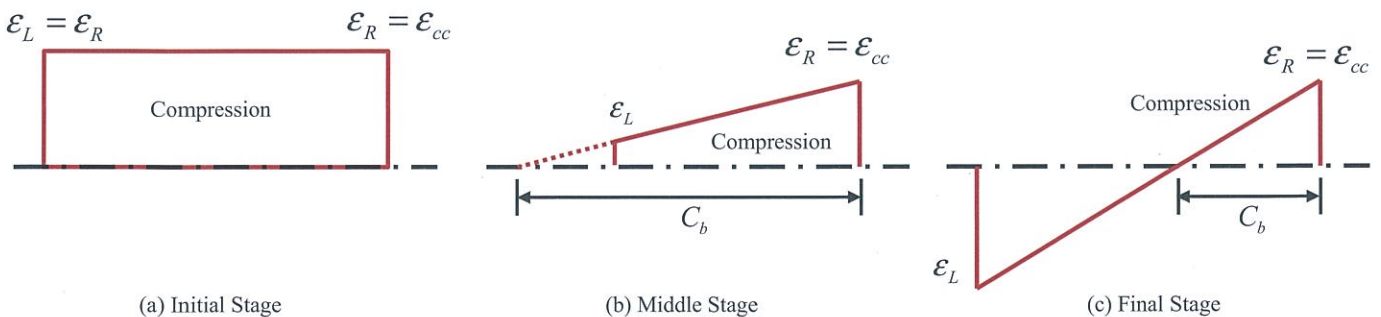


Fig. 5c. Stages of strain distribution [2]

concrete stress-strain curve and elasto-plastic steel behaviour and b) confined concrete stress-strain curve and accounting for strain hardening of the steel. Fig. 5a shows the idealized section, Fig. 5b the stress-strain curves adopted for concrete and steel. The analysis is performed at the stage of strain distribution as shown in Fig. 5c. The stresses acting on the concrete, longitudinal reinforcement and inner tube are calculated for each stage of strain distribution. By summing them, the axial load and the moment are calculated for each stage of the strain distribution; P_j and M_j are given by Eqs. (1) and (2) respectively:

$$P_j = P_j^{CC} + P_j^{CV} + P_j^R + P_j^T \quad (1)$$

$$M_j = M_j^{CC} + M_j^{CV} + M_j^R + M_j^T \quad (2)$$

where:

P_j axial load acting at j th stage of strain contribution
 P_j^{CC} axial load acting on core concrete at j th stage of strain contribution

P_j^{CV} axial load acting on cover concrete at j th stage of strain contribution
 P_j^R axial load acting on longitudinal reinforcement at j th stage of strain contribution
 P_j^T axial load acting on inner tube at j th stage of strain contribution
 M_j moment at j th stage of strain contribution
 M_j^{CC} moment acting on core concrete at j th stage of strain contribution
 M_j^{CV} moment acting on cover concrete at j th stage of strain contribution
 M_j^R moment acting on longitudinal reinforcement at j th stage of strain contribution
 M_j^T moment acting on inner tube at j th stage of strain contribution

The calculation procedure for the axial force-bending moment interaction for investigating the fire resistance performance of ICH RC column is shown in Fig. 6. After deducting the material properties in the ICH RC column

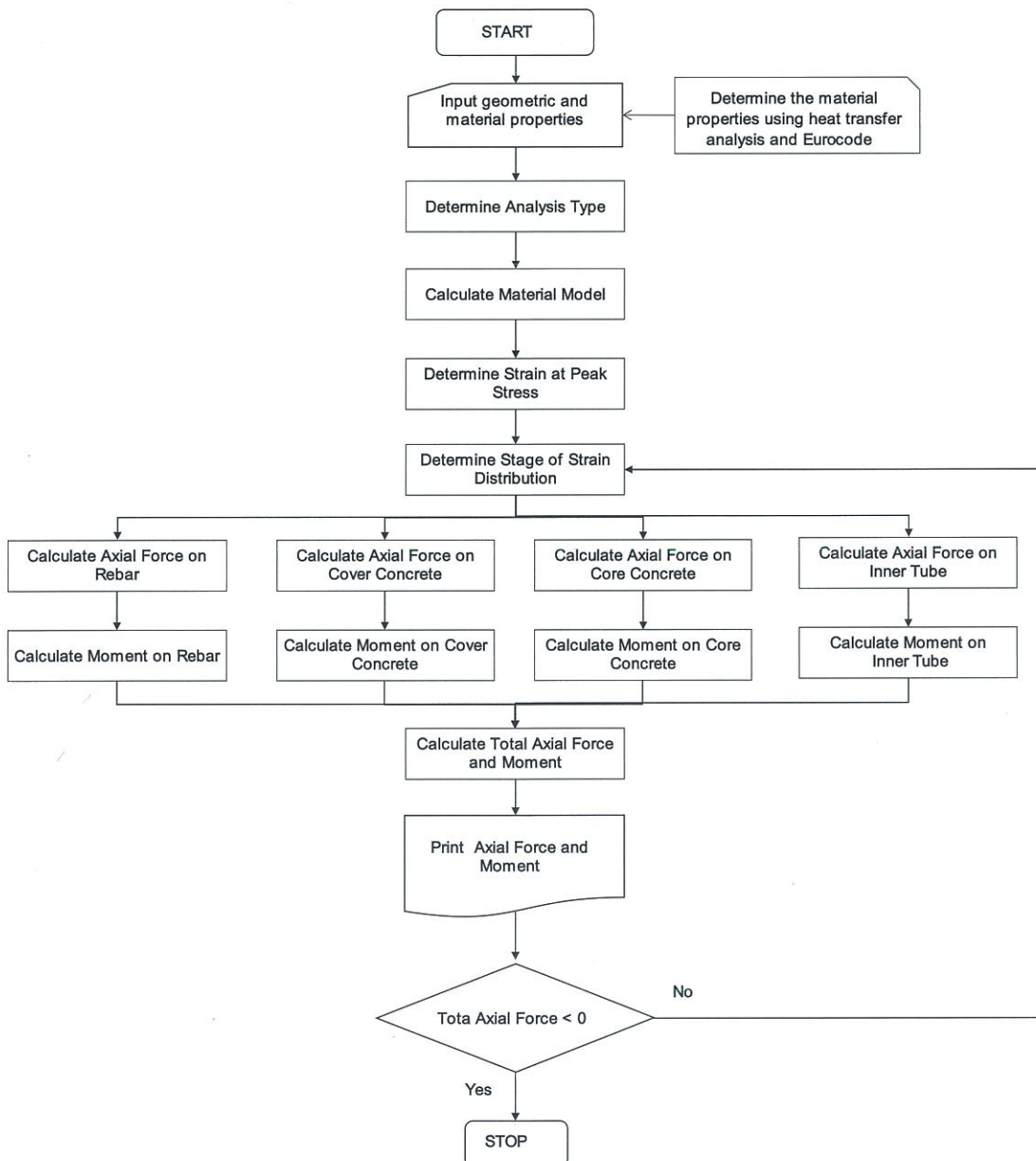


Fig. 6. Calculation procedure for axial load-bending moment interaction analyses [2]

using heat transfer analysis and the Eurocode, the material model and strain at peak stress are calculated. Interaction between axial force and bending moment can be calculated using the method suggested by Han et al. [2].

2.3 Heat transfer analysis and verification for application

In this study, a heat transfer analysis was performed in ABAQUS [9] to investigate the conduction of heat in terms of fire time after the onset of a fire. The basic energy balance for heat transfer analysis uses the theory of Green and Naghdi [9], expressed as Eq. (3). It is assumed that thermal and mechanical problems are uncoupled in the sense that $U = U(\theta)$ only.

$$\int_V \rho \dot{U} dV = \int_s q ds + \int_V r dV \tag{3}$$

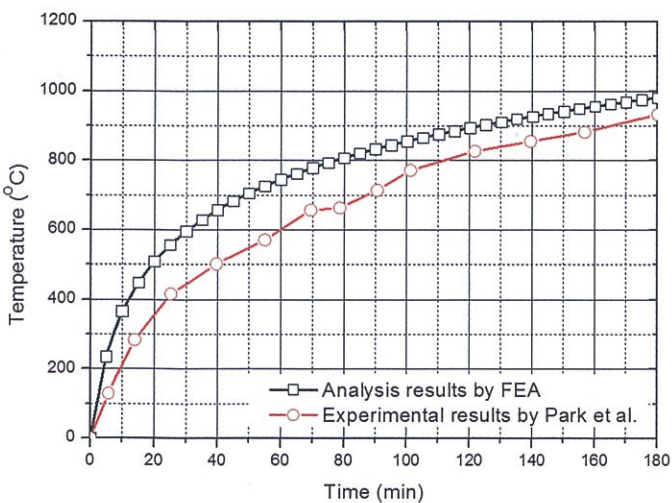
where:

- V volume of solid material of surface area S
 - ρ density of the material
 - \dot{U} material time rate of internal energy
 - q heat flux per unit area of the body flowing into the body
 - r external heat supplied to the body per unit volume
 - θ temperature of the material
- (q and r do not depend on the strain or displacement of the body)

DC2D4, a four-node linear heat transfer element, is used for representing steel and concrete. Furthermore, the thermal material properties for heat transfer analysis in a fire are the same as those described in the previous section. The average furnace temperature, measured using the thermocouples specified in the cotton pad test, is monitored and controlled such that it follows the relationship given by Eq. (4). This thermal load is applied uniformly to the column surface.

$$T = 345 \log_{10}(8t + 1) + 20 \tag{4}$$

where T denotes the average furnace temperature in °C and t the time in minutes.



(a) Temperature on outer concrete face

Fig. 9. Temperature of DSCCT column

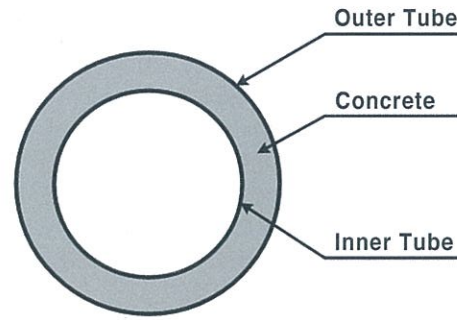


Fig. 7. Section through DSCCT column [10]

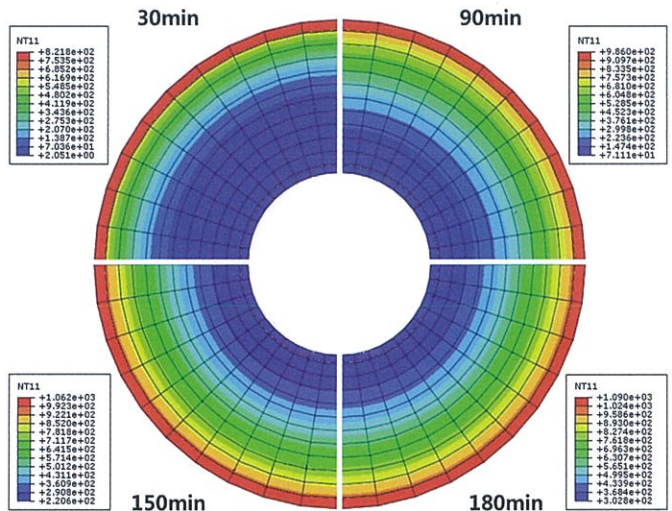
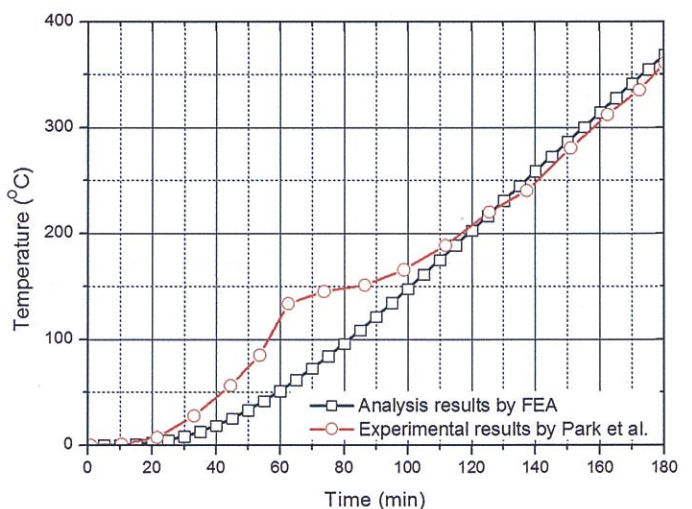


Fig. 8. Heat transfer analysis results of DSCCT column

Table 1. Dimensions of DSCCT column for verifying analysis method [9]

| | |
|---------------------------------|-------|
| Diameter of column (mm) | 406.4 |
| Thickness of outer tube (mm) | 9 |
| Thickness of inner tube (mm) | 7.1 |
| Diameter of hollow section (mm) | 150 |



(b) Temperature at D/4 of column

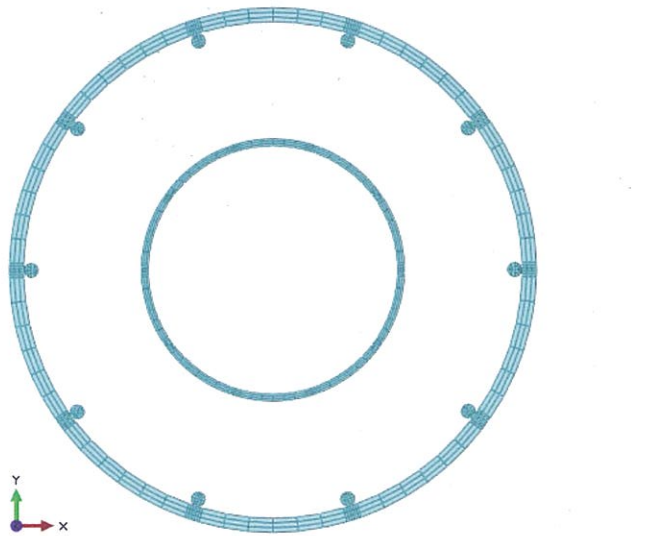
This heat transfer analysis method should be verified before applying it to the ICH RC column. In this paper, the analysis method is verified indirectly using another type of column as summarized and shown in Table 1 and Fig. 7 respectively because an experimental study of an ICH RC column in a fire has not yet been conducted. The dimensions of the double-skin composite tubular (DSCT) column, including those of the outer tube, concrete and inner tube, are listed in Table 1. The fire test was performed under an ISO 834 standard fire by Park et al. [10].

The heat transfer analysis is performed using the suggested thermal material properties and the DSCT column dimensions listed in Table 1. Fig. 8 shows the temperature distribution in the column during fire time at 30 min intervals. Fire heat is conducted to the hollow face from the surface of the outer tube. Figs. 9a and 9b show a comparison of the temperature changes at the outer surface of the concrete and D/4 of the diameter, as obtained in the heat transfer analysis performed in this study. The figures indicate that as time passes, the temperatures at outer concrete surface and D/4 of column diameter in-

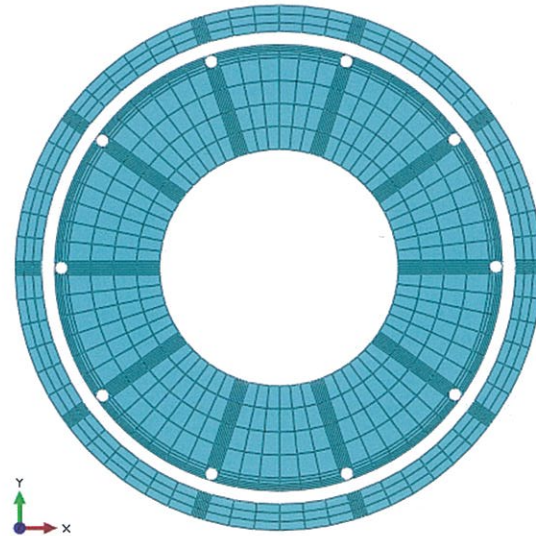
crease gradually, and the tendency for a temperature rise as obtained through heat transfer analysis is similar to that obtained experimentally [10]. The comparison results show that the analysis method is reasonable; thus, it can be used for investigating the conduction of fire heat in ICH RC columns comprising concrete, inner tube and steel reinforcement.

3 Fire resistance of ICH RC column

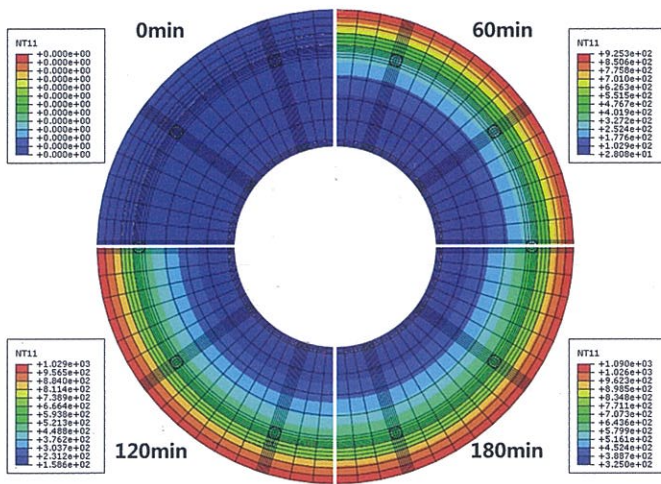
In this section, the heat transfer analysis of an ICH RC column under the ISO 834 standard fire [4] is performed using the FEA method verified in the previous section. Changes to the structural properties of the ICH RC column's component elements are derived based on the temperatures obtained from the heat transfer analysis. The compression and moment performance of the ICH RC column in terms of fire time are investigated. In addition, parametric studies are performed by selecting main parameters such as hollow ratio, depth of cover concrete and thickness of inner tube.



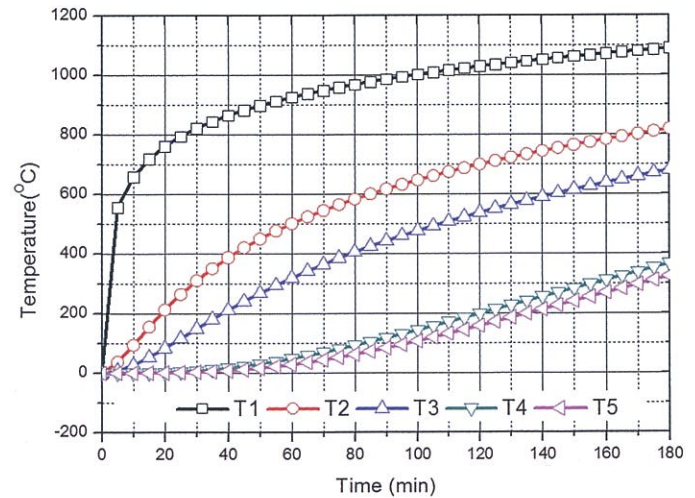
(a) Modelling of transverse reinforcement, longitudinal reinforcement and inner tube



(b) Modelling of cover concrete and core concrete



(c) Temperature distribution in ICH RC column in terms of fire time



(d) Temperature at each location

Fig. 10. Modelling of and temperature distribution in ICH RC column

3.1 Heat transfer analysis and behaviour of ICH RC column under ISO 834 standard fire

Table 2 lists the dimensions of the ICH RC column used for the heat transfer analysis. The diameter of the column is 400 mm, its hollow ratio is 0.5 and the thickness of the inner tube is 5 mm. Here, the hollow ratio is the ratio of the outer diameter of the transverse reinforcement to the inner diameter of the concrete. The thermal material properties given in section 2.1 are used for the heat transfer analysis. The type of element used for representing concrete, reinforcement and inner tube in the heat transfer analysis is DC2D4, a four-node, linear, solid element. Furthermore, ISO 834 standard fire [4] was applied as the thermal load on the surface of the ICH RC column.

All components are modelled individually. Fig. 10a shows the modelling of transverse reinforcement, longitudinal reinforcement and inner tube. Concrete is modelled as shown Fig. 10b. Fig. 10c shows the temperature distribution in the ICH RC column in terms of fire time at

60 min intervals. Fire heat is conducted to the inside of the ICH RC column with fire exposure time. Here, T1 denotes the surface of the cover concrete, T2 and T3 the transverse and longitudinal reinforcement respectively, T4 the concrete centre and T5 the inner tube. The change in temperature at each location is as shown in Fig. 10d. As the conductivity of concrete is very low, the cover concrete and core concrete delay fire heat conduction to the inside of the column. Therefore, the temperature at the centre of the core concrete is similar to the temperature of the inner tube, as shown in Fig. 10d.

Next, the structural behaviour of the ICH RC column under the ISO 834 standard fire is evaluated using structural material properties in terms of temperature, as shown in Fig. 4. Temperature by fire time is based on the results of the heat transfer analysis, and the structural material properties of the ICH RC column at room temperature are listed Table 3. These are standard values.

Tables 4–7 show the changes in the structural material properties of the ICH RC column components during a

Table 2. Dimensions of ICH RC column

| | |
|---|-----|
| Diameter of column (mm) | 400 |
| Thickness of cover concrete (mm) | 20 |
| Diameter of transverse reinforcement (mm) | 10 |
| Diameter of longitudinal reinforcement (mm) | 10 |
| Number of longitudinal reinforcing bars | 10 |
| Outer diameter of concrete (mm) | 340 |
| Inner diameter of concrete (mm) | 180 |
| Thickness of inner tube (mm) | 5 |

Table 3. Material properties of ICH RC column at room temperature

| | |
|--|---------|
| Compressive strength of concrete (MPa) | 30 |
| Yield strength of steel reinforcement (MPa) | 400 |
| Elastic modulus of steel reinforcement (MPa) | 200 000 |
| Yield strength of steel tube (MPa) | 320 |
| Elastic modulus of steel tube (MPa) | 210 000 |

Table 4. Material properties of longitudinal reinforcement based on fire time

| Time (min) | Average yield strength (MPa) | Average ultimate strength (MPa) | Average elastic modulus (MPa) |
|------------|------------------------------|---------------------------------|-------------------------------|
| 0 | 400.00 | 500.00 | 200 000.00 |
| 30 | 400.00 | 500.00 | 190 416.70 |
| 60 | 400.00 | 481.81 | 156 362.20 |
| 90 | 364.02 | 364.02 | 131 821.60 |
| 120 | 270.68 | 270.68 | 100 670.63 |
| 150 | 181.29 | 181.29 | 59 484.50 |
| 180 | 122.55 | 122.55 | 37 457.72 |

Table 5. Material properties of transverse reinforcement based on fire time

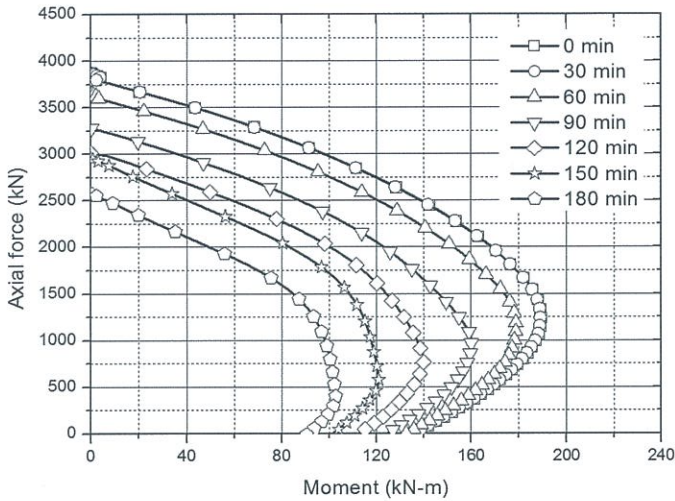
| Time (min) | Average yield strength (MPa) | Average ultimate strength (MPa) | Average elastic modulus (MPa) |
|------------|------------------------------|---------------------------------|-------------------------------|
| 0 | 400.00 | 500.00 | 200 000.00 |
| 30 | 400.00 | 490.55 | 158 109.20 |
| 60 | 311.88 | 311.88 | 119 944.32 |
| 90 | 173.39 | 173.39 | 56 522.60 |
| 120 | 95.10 | 95.10 | 27 163.88 |
| 150 | 63.28 | 63.28 | 21 214.12 |
| 180 | 41.75 | 41.75 | 17 493.64 |

Table 6. Material properties of core concrete based on fire time

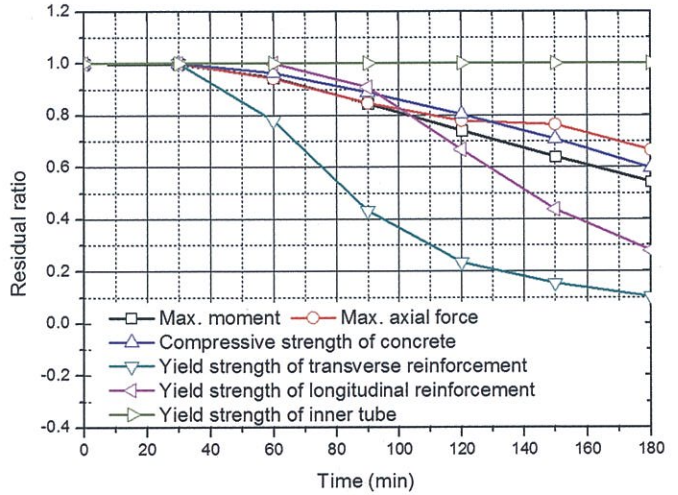
| Time (min) | Average compressive strength (MPa) | Average elastic modulus (MPa) |
|------------|------------------------------------|-------------------------------|
| 0 | 30.00 | 28 577 |
| 30 | 30.00 | 28 577 |
| 60 | 29.08 | 28 577 |
| 90 | 27.20 | 28 072 |
| 120 | 24.72 | 25 735 |
| 150 | 22.24 | 23 314 |
| 180 | 18.83 | 20 949 |

Table 7. Material properties of inner tube based on fire time

| Time (min) | Average yield strength (MPa) | Average ultimate strength (MPa) | Average elastic modulus (MPa) |
|------------|------------------------------|---------------------------------|-------------------------------|
| 0 | 320.00 | 400.00 | 210 000.00 |
| 30 | 320.00 | 400.00 | 210 000.00 |
| 60 | 320.00 | 400.00 | 210 000.00 |
| 90 | 320.00 | 400.00 | 210 000.00 |
| 120 | 320.00 | 400.00 | 197 685.81 |
| 150 | 320.00 | 400.00 | 180 293.09 |
| 180 | 320.00 | 380.02 | 162 755.36 |



(a) P-M interaction diagram for section



(b) Residual strength ratio in ICH RC column components

Fig. 11. Behaviour of ICH RC column based on fire time

fire. The material properties of steel and concrete based on fire exposure times were set as shown in Fig. 4.

Table 4 lists the material properties of the longitudinal reinforcement based on fire exposure time. Close to 90 min, the average yield strength of the longitudinal reinforcement begins to decline. It drops from 500 to 122 MPa at about 180 min. Furthermore, the average ultimate strength and average elastic modulus reach 122.52 and 37457.72 MPa respectively.

The change rates of the material properties of the transverse reinforcement are larger than those for the longitudinal reinforcement, as shown in Fig. 4, because the transverse reinforcement is located outside the longitudinal reinforcement. At 180 min, the average yield and ultimate strength are both 41.75 MPa.

Table 6 shows the changes in the average compressive strength and average elastic modulus of the core concrete. Here, the average compressive strength of the core concrete decreased gradually from 30 to 18.83 MPa over the fire exposure time of 180 min. Material properties of the inner tube exhibit few decreasing rates because it is located inside the core concrete. Furthermore, the temperature of the inner tube was about 300 °C at 180 min. Table 7 lists the structural material properties of the inner tube by fire time. Only the average elastic modulus changes because it is located inside the core concrete, which delays the conduction of fire heat.

Table 8. Dimensions of analysis models by hollow ratio

| Hollow ratio | 0.2 | 0.3 | 0.4 | 0.5 | 0.6 | 0.7 |
|---|-----|-----|-----|-----|-----|-----|
| Diameter of hollow section (mm) | 62 | 98 | 134 | 170 | 206 | 242 |
| Thickness of cover concrete (mm) | 20 | | | | | |
| Diameter of transverse reinforcement (mm) | 10 | | | | | |
| Thickness of inner tube (mm) | 5 | | | | | |
| Diameter of longitudinal reinforcement (mm) | 10 | | | | | |
| Number of longitudinal reinforcing bars | 10 | | | | | |
| Diameter of column (mm) | 400 | | | | | |

The performance of the ICH RC column is evaluated using changes to the structural material properties of the components, which are listed in Tables 4–7. The P-M interaction diagram of the ICH RC column, shown in Fig. 11a, is drawn for 30 min intervals. Axial and moment performance decreases as fire exposure time passes. The residual strength, axial strength and moment performance of the ICH RC column are compared in Fig. 11b. The change rates of the maximum moment and maximum axial performance show similar tendencies to the change rate of the core concrete’s compressive strength.

3.2 Parametric studies

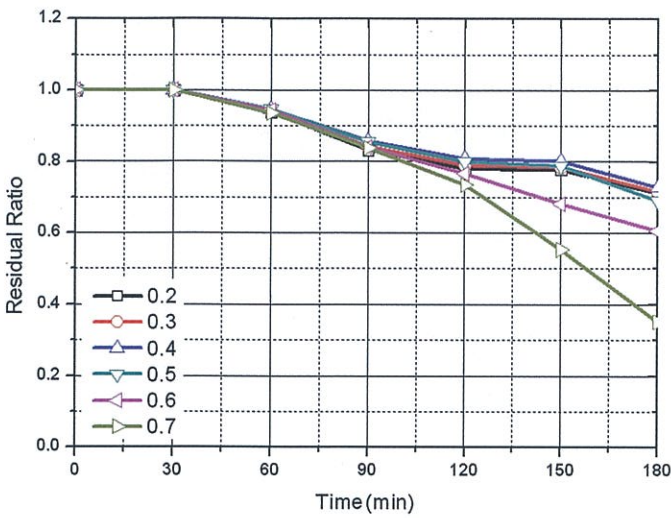
In this section, the fire resistance performance of the ICH RC column is investigated through parametric studies considering hollow ratio, thickness of cover concrete and thickness of inner tube. The fire resistance of the ICH RC column is evaluated through parametric studies based on the method suggested in the preceding section.

3.2.1 Hollow ratio

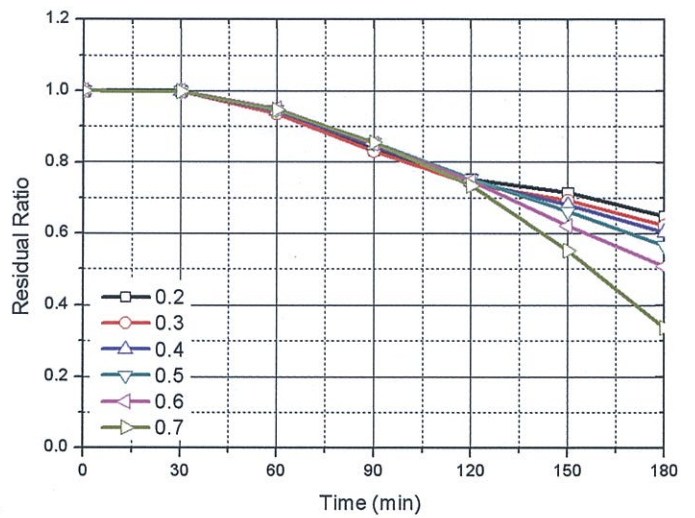
Table 8 lists the dimensions of the analysis models in terms of hollow ratio, i.e. ratio of core concrete outer and inner diameters. The effect of the hollow ratio is investi-

gated by varying it from 0.2 to 0.7, whereas the other dimensions of the analysis models are maintained at their original values.

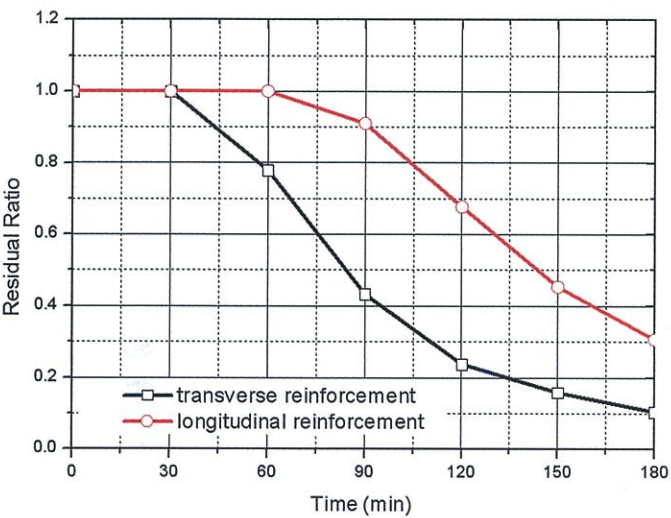
Figs. 12a and b show the residual maximum moment ratio and residual maximum axial force ratio respectively. The hollow ratio is changed from 0.2 to 0.7, which degrades



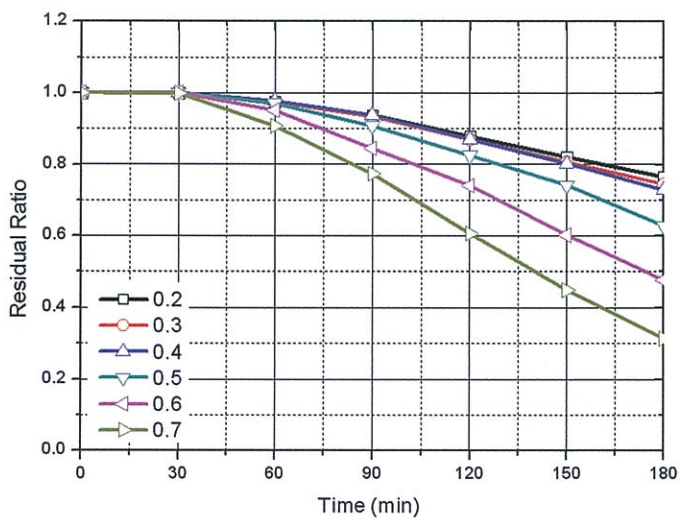
(a) Residual maximum moment ratio



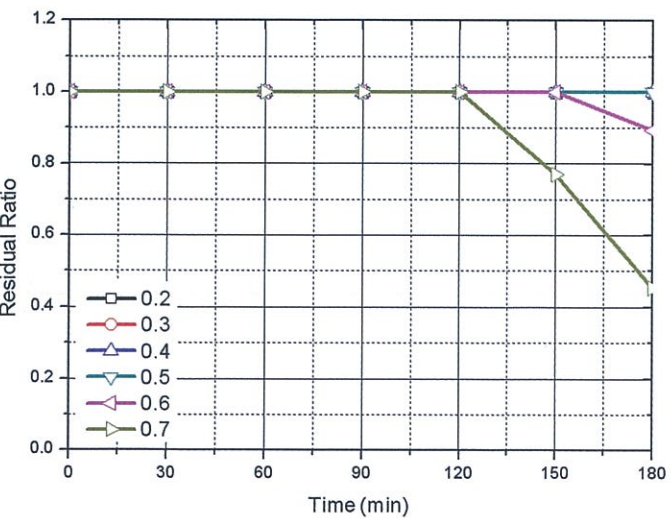
(b) Residual maximum axial force ratio



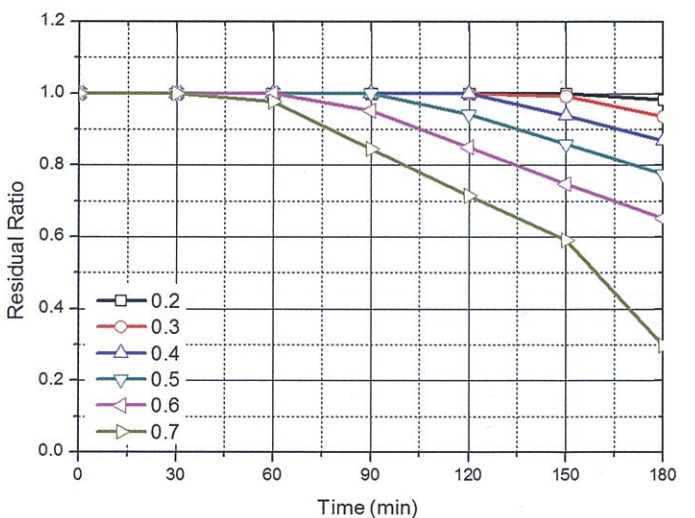
(c) Residual yield strength ratio of transverse and longitudinal reinforcement



(d) Residual compressive strength ratio of core concrete



(e) Residual yield strength ratio of inner tube

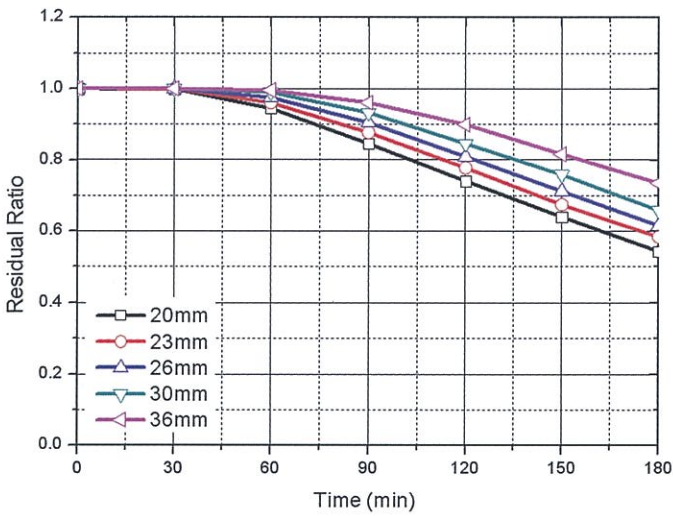


(f) Residual elastic modulus ratio of inner tube

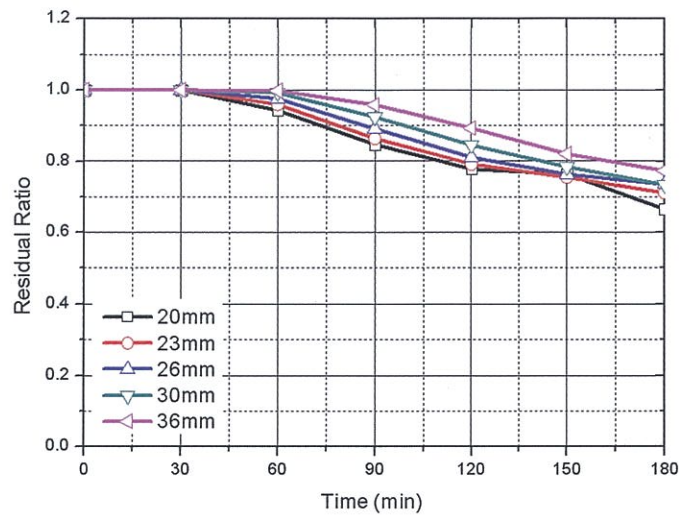
Fig. 12. Residual strength ratio of ICH RC column by hollow ratio

column performance. This behaviour of the ICH RC column is ascribed to the effect of the core concrete. The tendency of the core concrete's residual compressive strength

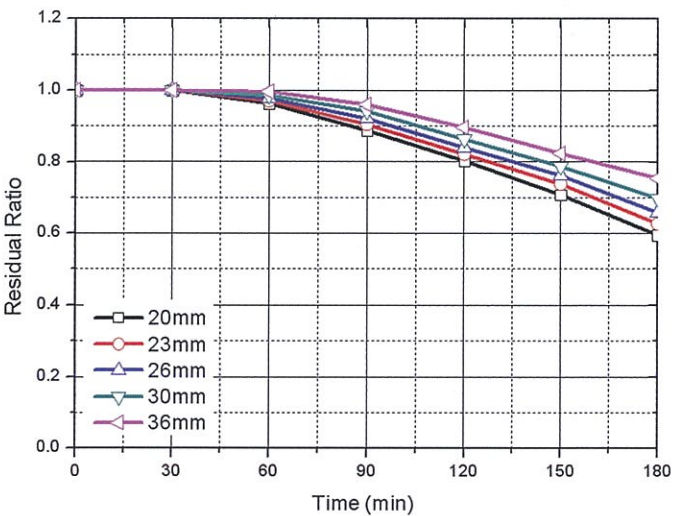
ratio is similar to those of the residual moment and the axial force ratio, as shown in Fig. 12d. Damage to the ICH RC column due to fire increases as the hollow ratio in-



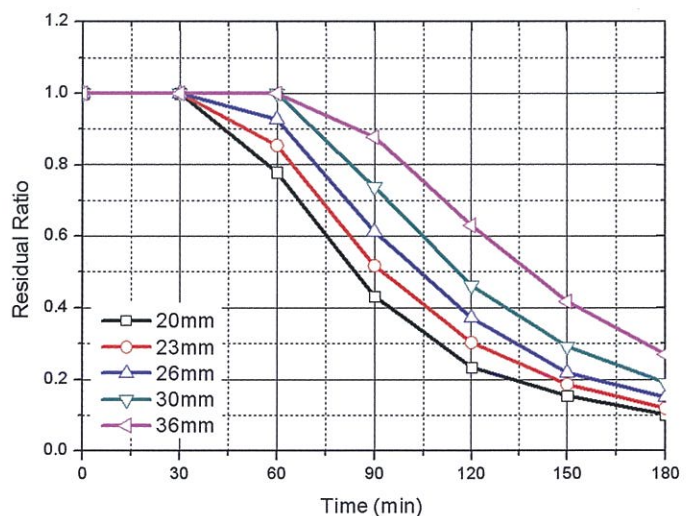
(a) Residual maximum moment ratio



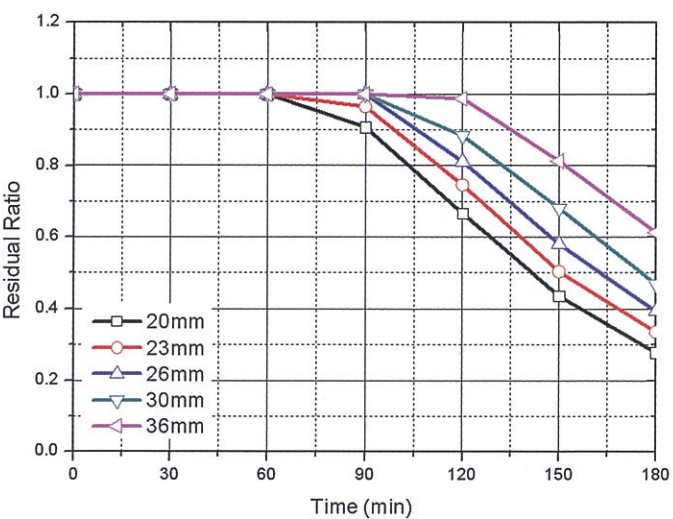
(b) Residual maximum axial force ratio



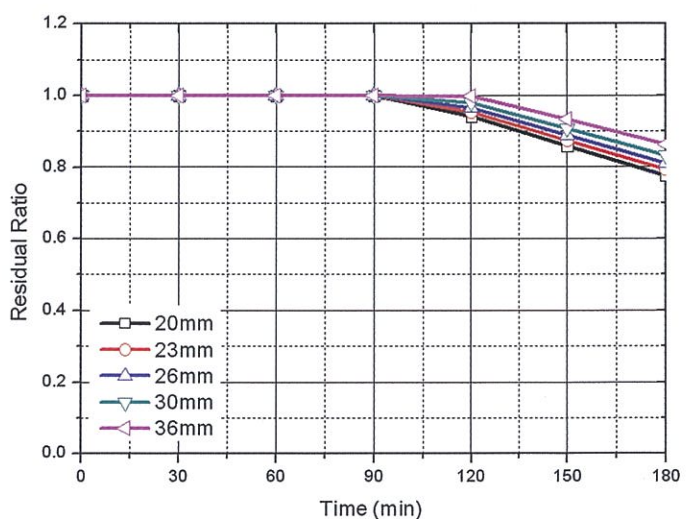
(c) Residual compressive strength ratio of core concrete



(d) Residual yield strength ratio of transverse reinforcement



(e) Residual yield strength ratio of longitudinal reinforcement



(f) Residual elastic modulus ratio of inner tube

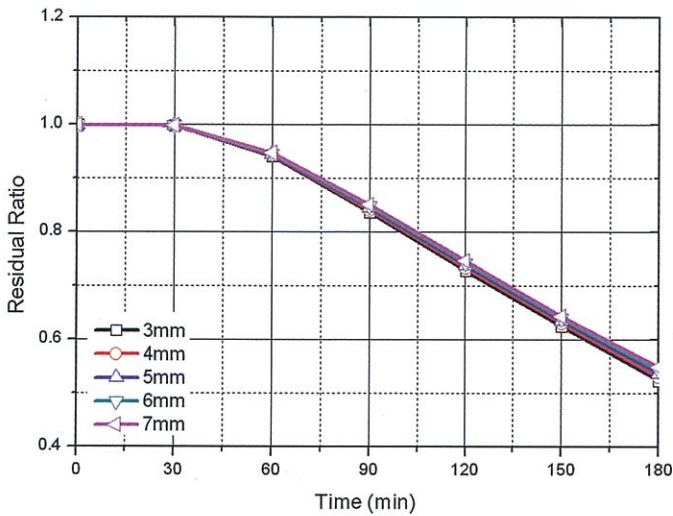
Fig. 13. Residual strength ratio of ICH RC column by thickness of cover concrete

creases because the thickness of the core concrete decreases. In addition, the residual yield strength ratio of the transverse and longitudinal reinforcement decreases, as shown in Fig. 12c. The residual ratio of all the models is

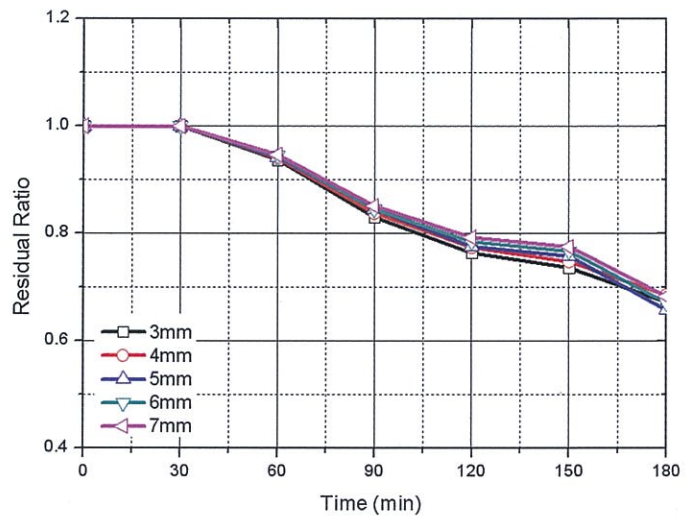
identical because only the inner diameter of the core concrete is changed. Additionally, the yield strength of the inner tube does not decrease despite its temperature reaching 300 °C owing to the fire.

Table 9. Dimensions of analysis models based on cover concrete thickness

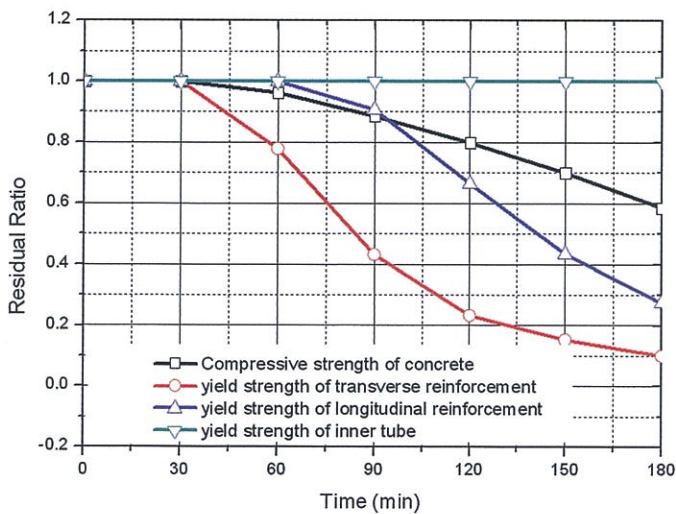
| | | | | | | |
|---|-----|----|----|----|----|----|
| Thickness of cover concrete (mm) | 20 | 23 | 26 | 30 | 36 | 20 |
| Hollow ratio | 0.5 | | | | | |
| Diameter of transverse reinforcement (mm) | 10 | | | | | |
| Thickness of inner tube (mm) | 5 | | | | | |
| Diameter of longitudinal reinforcement (mm) | 10 | | | | | |
| Number of longitudinal reinforcing bars | 10 | | | | | |
| Diameter of column (mm) | 400 | | | | | |
| Diameter of hollow section (mm) | 170 | | | | | |



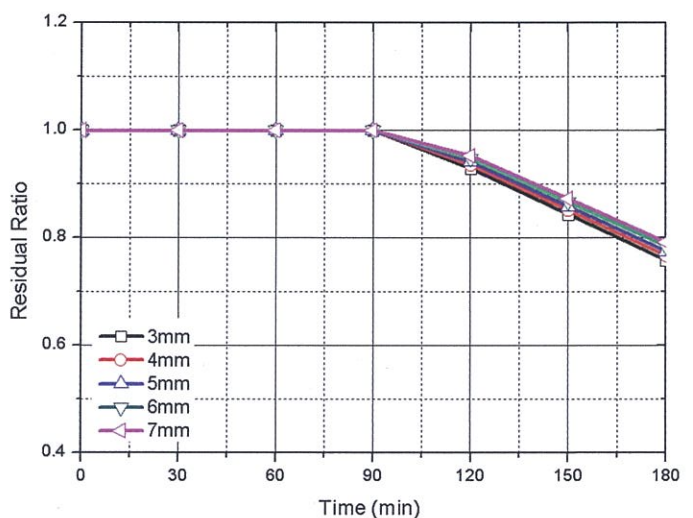
(a) Residual maximum moment ratio



(b) Residual maximum axial force ratio



(c) Comparison of residual strength ratio



(d) Residual elastic modulus ratio of inner tube

Fig. 14. Residual strength ratio of ICH RC column by thickness of inner tube

Table 10. Dimensions of analysis models based on inner tube thickness

| Thickness of inner tube (mm) | 3 | 4 | 5 | 6 | 7 |
|---|-----|-----|-----|-----|-----|
| Diameter of hollow section (mm) | 164 | 168 | 170 | 172 | 174 |
| Hollow ratio | 0.5 | | | | |
| Diameter of transverse reinforcement (mm) | 20 | | | | |
| Thickness of cover concrete (mm) | 10 | | | | |
| Diameter of longitudinal reinforcement (mm) | 10 | | | | |
| Number of longitudinal reinforcing bars | 10 | | | | |
| Diameter of column (mm) | 400 | | | | |

3.2.2 Thickness of cover concrete

Next, the thickness of the cover concrete is varied for investigating the fire resistance of the ICH RC column, as summarized in Table 9. It is changed from 20 to 36 mm, whereas the other dimensions of the models are maintained at their original values.

Figs. 13a and b show, respectively, the residual moments and the axial force of the ICH RC column. The damage rate of the ICH RC column decreases as the thickness of the cover concrete increases. The cover concrete delays the conduction of fire heat. As shown in Figs. 13d and e, the transverse and longitudinal reinforcement reach a high temperature and their yield strength decreases rapidly because they are located outside the column, unlike the cover concrete. If the confining effect of the transverse reinforcement on the concrete is considered, the strength of the confined concrete would decrease rapidly because reduction of the yield strength of the transverse reinforcement. In addition, the elastic modulus of the inner tube decreases slowly after 90 min.

3.2.3 Thickness of inner tube

Table 10 lists the dimensions of the analysis models in terms of the inner tube thickness, which is changed from 3 to 7 mm in steps of 1 mm. Other dimensions of the analysis models are maintained at their original values.

As shown in Fig. 14, the rate of decrease of the residual strength falls as the thickness of the inner tube is increased from 3 to 7 mm. However, the yield strength of the inner tube does not decrease, as shown in Fig. 14c. This improvement in performance is an effect of increasing the inner tube thickness.

4 Summary and conclusions

In this study, the fire resistance performance of an ICH RC column was investigated using an analytical Eurocode method. In addition, the effects of changing hollow ratio, thickness of inner tube and thickness of cover concrete on fire resistance performance were analysed. The following conclusions can be drawn:

(1) As the hollow ratio is increased, so the fire resistance performance improves. This behaviour of the ICH RC

column is ascribed to the effect of the core concrete. The residual compressive strength ratio of the core concrete has a tendency similar to those of the residual moment and the axial force ratio. Damage to an ICH RC column by fire increases as the hollow ratio increases, which is ascribed to a decrease in core concrete thickness.

- (2) The damage rate of an ICH RC column decreases as the cover concrete thickness increases because the cover concrete retards the conduction of fire heat. Therefore, the fire resistance performance of an ICH RC column can be improved by increasing the cover concrete thickness.
- (3) The fire resistance performance of an ICH RC column suffers as the thickness of the inner tube is decreased. The reduced performance is a result of decreasing the inner tube thickness.

Acknowledgments

This research was financially supported by the Korea Institute of Ocean Science & Technology (KIOST), project No. PE99274 & PE99223.

References

1. Han, T. H., Lim, N. H., Han, S. Y., Park, J. S., Kang, Y. J.: Non-linear concrete model for an internally confined hollow reinforced concrete column. *Mag Concr Res*, 60(6) (2008), pp. 429–440.
2. Han, T. H., Yoon, K. Y., Kang, Y. J.: Compressive strength of circular hollow reinforced concrete confined by an internal steel tube. *Construction and Building Materials* 24(9) (2010), pp. 1690–1699.
3. Xiao, J., Fan, Y., Tawana, M. M. (2013), Residual compressive and flexural strength of a recycled aggregate concrete following elevated temperatures. *Structural Concrete*, 14: 168–175.
4. ISO 834: Fire Resistance Tests – Elements of Building Construction (1999).
5. Eurocode 2: Design of concrete structures – Part 1.2: General rules – Structural fire design, EN 1992-1-2. CEN, Brussels, 2004.
6. Eurocode 3: Design of steel structures – Part 1–2: General rules – Structural fire design, EN 1993-1-2. CEN, Brussels, 2005.

7. Committee Euro-International Du Beton: Fire Design of Concrete Structures in accordance with CEB/FIP Model Code 90 (final draft), CEB Bulletin.
8. *Kilpatrick, A. E., Ranagan B. V.*: Deformation-control analysis of composite concrete columns. School of Civil Engineering, Curtin University of Technology, Perth, Western Australia. Research Report No. 3/97 (1997).
9. SIMULIA (2010), ABAQUS Manual 6.9.1.
10. *Park, S. H., Song, K. C., Chung, S. K., Min, B. Y., Choi, S. M.*: An Experimental Study on the Fire Resistance of Concrete-filled Double Skin Tubular Columns. 5th Int. Symposium on Steel Structures (2009), pp. 299–307.



Deok Hee Won Ph.D
Ph.D., Research Scientist at Coastal Development & Ocean Energy Research Division, Korea Institute of Ocean Science and Technology, Ansan, 426-744, Republic of Korea



Woo Sun Park Ph.D
Ph.D., Principal Research Scientist at Coastal Development & Ocean Energy Research Division, Korea Institute of Ocean Science and Technology, Ansan, 426-744, Republic of Korea



In-Sung Jang Ph.D
Ph.D., Principal Research Scientist at Coastal Development & Ocean Energy Research Division, Korea Institute of Ocean Science and Technology, Ansan, 426-744, Republic of Korea



Sang-Hun Han Ph.D
Ph.D., Principal Research Scientist at Coastal Development & Ocean Energy Research Division, Korea Institute of Ocean Science and Technology, Ansan, 426-744, Republic of Korea



Taek Hee Han Ph.D
Ph.D., Principal Research Scientist at Coastal Development & Ocean Energy Research Division, Korea Institute of Ocean Science and Technology, Ansan, 426-744, Republic of Korea